TITLE PAGE

Title:

Associations between Motor Unit Action Potential Parameters and Surface EMG Features

Authors:

Alessandro Del Vecchio[1,3], Francesco Negro[2], Francesco Felici[1] and Dario Farina[3]

Affiliations:

[1]Department of Movement, Human and Health Sciences, University of Rome "Foro Italico", 00135 Rome, Italy;

[2]Department of Clinical and Experimental Sciences, University of Brescia, 25123 Brescia, Italy;

[3]Department of Bioengineering, Imperial College London, London, UK

Corresponding author:

D. Farina. Department of Bioengineering, Imperial College London, London, UK. Email: d.farina@imperial.ac.uk

Key words

Surface electromyography; Motor unit; Recruitment; Conduction velocity; EMG features; Size principle

Acknowledgements

Alessandro Del Vecchio has received funding from the University of Rome "Foro Italico". Francesco Negro has received funding from the European Union's Horizon 2020 research and innovation programme under the Marie Skłodowska-Curie grant agreement No 702491 (NeuralCon).

ABSTRACT

The surface interference EMG signal provides some information on the neural drive to muscles. However, the association between neural drive to muscle and muscle activation has long been debated with controversial indications due to the unavailability of motor unit population data. In this study, we clarify the potential and limitations of interference EMG analysis to infer motor unit recruitment strategies with an experimental investigation of several concurrently active motor units and of the associated features of the surface EMG. For this purpose, we recorded high-density surface EMG signals during linearly increasing force contractions of the tibialis anterior muscle, up to 70% of maximal force. The recruitment threshold (RT), conduction velocity (MUCV), median frequency (MDF_{MU}) and amplitude (RMS_{MU}) of action potentials of 587 motor units from 13 individuals were assessed and associated to features of the interference EMG. MUCV was positively associated with RT (R^2 = 0.64 ± 0.14) whereas MDF_{MU} and RMS_{MU} showed a weaker relation with RT (R^2 = 0.11 ± 0.11; 0.39 ± 0.24, respectively). Moreover, the changes in average conduction velocity estimated from the interference EMG predicted well the changes in MUCV (R^2 = 0.71), with a strong association to ankle dorsi-flexion force (R^2 = 0.81 ± 0.12). Conversely, both the average EMG MDF and RMS were poorly associated to motor unit recruitment. These results clarify the limitations of EMG spectral and amplitude analysis in inferring the neural strategies of muscle control and indicate that, conversely, the average conduction velocity could provide relevant information on these strategies.

New and Noteworthy

The surface EMG provides information on the neural drive to muscles. However, the associations between EMG features and neural drive have been long debated due to unavailability of motor unit population data. Here, by using novel highly-accurate decomposition of the EMG, we related motor unit population behavior to a wide range of voluntary forces. The results fully clarify the potential and limitation of the surface EMG to provide estimates of the neural drive to muscles.

INTRODUCTION

The generation of force is accomplished by the concurrent recruitment and modulation of the discharge rate of motor units. Motor units are recruited orderly according to the size of the motor neurons (31). When motor neurons discharge action potentials, a local depolarization at the neuromuscular junction generates action potentials in the innervated muscle fibers. This connection creates a one-to-one relation between axonal and muscle fiber action potentials (30).

When an array of electrodes is placed in the direction of the muscle fibers, it is possible to observe and measure the propagation of action potentials from the neuromuscular junction to the tendon, with a velocity that ranges between 2 and 6 m/s (3). The average propagation velocity of action potentials along muscle fibers (muscle fiber conduction velocity, MFCV) can be measured in vivo during voluntary contractions from an interference EMG signal and represents the weighted mean of conduction velocities of the active muscle fibers. The interference EMG signal can also be processed to extract features, such as its amplitude (e.g., root mean square, RMS) and power spectral components (e.g., Mean/Median frequency, MNF/MDF) (24, 25). These variables are often referred to as global EMG features because they represent the activity of all active motor units and not individual motor unit properties. The conduction velocity of the fibers in individual motor units (MUCV) can be measured by decomposing the EMG signals and extracting the action potentials for isolated motor units (15, 45). Amplitude and power spectral features may be used to further characterize the decomposed action potentials of individual units.

With respect to EMG decomposition and the study of individual motor units, the global EMG analysis can be applied to a broader range of experimental conditions (e.g., dynamic contractions, explosive contractions, gait analysis). Therefore, the relations between global EMG variables that represent muscle activation and the neural drive to muscle (individual motor unit discharge timings) have been investigated with simulation models and experimentally (6, 19, 24, 58). In these studies, the feasibility and reliability of associating global EMG variables to the underlying behavior of the active units have been extensively debated. Despite it has been shown that these associations are weak (17, 21, 37), global EMG analysis is still often used for indirectly inferring the type of recruited motor units (e.g., (28, 34, 40, 41, 54, 57, 59, 62). This approach is sometimes justified by the fact that criticisms on the use of global EMG variables for assessing the neural strategies are mainly based on simulation work that may provide different results depending on tuning of model parameters (13, 40, 61). There are indeed no systematic studies that experimentally reported the relations between global EMG variables and the behavior of large groups of concurrently active motor units. The difficulty of these investigations is the identification of the activity of relatively large populations of motor units, as it is needed to investigate the association between neural drive to muscles and global EMG variables.

Recently, it has become possible to concurrently identify several motor units by high-density EMG decomposition (27, 49, 50), as opposed to the small number of motor units that can be studied with selective intramuscular recordings. These techniques allow us for the first time to assess the extent to which information about the neural drive to the muscle can be extracted from recordings of muscle activation during a large range of voluntary forces in the tibialis anterior muscle. The results fully clarify the potentials and limitations in the use of global surface EMG analysis for studying the neural control of muscle activation.

METHODS

Thirteen healthy, recreationally active young men (mean (SD), 24.6 (2.6) yr, 180 (5.8) cm, 80 (6.3) kg) were recruited and completed the experiment that was approved by the Ethical Committee of the Universitätmedizin Göttingen (approval n. 1/10/12). None of the subjects reported any history of neuromuscular disorders or previous lower limb surgery. An informed consent form was signed by all the volunteers before participating in the experiments.

Experimental procedure

The subjects were familiarized with the experimental conditions before participating in the testing procedures. The experimental conditions consisted of a series of isometric maximal and submaximal ankle dorsi-flexions. The contractions were completed in the following order: isometric maximal voluntary force contractions (MVC) and isometric ramp contractions. Participants completed three MVC separated by at least 30s, during which they were instructed to “push as hard as possible” for at least 3 s. The greatest force produced during any of the

MVCs was considered as the maximum voluntary contraction (MVC) force. The MVC measure was followed by contractions during which the force increased at the rate of 5% MVC/s^{-1} to reach target forces of either 35, 50, and 70% MVC, which were sustained for 10 s. The volunteers completed a total of six contractions of this type, two for each target force. The contractions were performed in randomized order and were separated by 5 min of rest.

Force and electromyogram recordings

The participants were seated in the chair of a Biodex System 3 in an upright position (Biodex Medical Systems Inc., Shirley, NY, USA), with the dominant leg (self-reported) extended and the ankle flexed at ~30° with respect to the neutral position (0°), which allowed a comfortable and stable position. The ankle and the foot were tightly fastened by Velcro straps. The ankle strap was in series with a load cell that was positioned perpendicular to the lateral malleolus. The visual feedback on force was provided by a cursor displayed on a computer monitor. The participants were instructed to follow a trapezoidal force trajectory.

High density surface electromyography (HDEMG) signals were recorded from the tibialis anterior muscle with a grid of 64 electrodes (5 columns and 13 rows; gold coated; 1-mm diameter; 8-mm interelectrode distance; OT Bioelettronica, Torino, Italy; Fig 1). Before fixing the high-density grid, a dry electrode array of 16 electrodes (OT Bioelettronica, Torino, Italy) was used to identify the distal innervation zone of the tibialis anterior muscle. The array was moved in the distal portion of the tibialis anterior to estimate the direction of the muscle fibers that corresponded to the alignment that led to the observation of action potentials propagating along the array without substantial changes in waveform shape. The electrode position was performed following the anatomical description for the location of the distal innervation zone of the tibialis anterior muscles reported in (14–16). Specifically, once the distal innervation zone and the fiber direction were identified, the adhesive high-density grid was placed as indicated in Fig. 1, with the first 4 rows in correspondence to the innervation zone and the electrode columns aligned to the fiber direction. Before placement of the grid, the skin was shaved, when needed, lightly abraded and cleansed with 70% ethanol. The electrode-skin contact was improved by conductive paste (SpesMedica, Battipaglia, Italy). The HDEMG signals were recorded in monopolar recordings with a multichannel amplifier (3dB bandwidth, 10-500 Hz; EMG-USB2+ multichannel amplifier, OT Bioelettronica, Torino, Italy). The EMG and force signals were concurrently sampled at 2048 samples/s, with 12 bits per sample.

Interference EMG signal analysis

HDEMG signals were digitally band-pass filtered with a 20-500 Hz Butterworth filter. Double differential signals (DD-HDEMG) were obtained from the monopolar recordings along the fiber direction (columns of the grid). The DD-HDEMG recordings were then inspected and the six channels with the highest cross-correlation in propagation were selected. From these channels, we computed MFCV, median frequency (MDF), and root mean square amplitude (RMS) from intervals of 500 ms (Fig 1. B). The MFCV estimation was obtained with a multichannel maximum-likelihood algorithm that was previously shown to provide estimates with an associated standard deviation <0.1 ms^{-1} (26). The MDF was computed from an estimate of the power spectrum based on the periodogram (23). The values of RMS and MDF estimated from the six DD-HDEMG channels used for MFCV estimation were averaged. Moreover, bipolar RMS and MDF signals were also derived from a bipolar recording with larger electrodes. For this purpose, the monopolar signals from two sets of five neighbor electrodes in the grid (with the central electrodes corresponding to those used for global MFCV analysis) were averaged to derive an approximation of two EMG signals recorded by large electrodes. These two EMG signals were differentiated to obtain a bipolar derivation with an interelectrode distance of 1.6 cm. This derivation will be referred to as large bipolar EMG.

Motor unit analysis

HDEMG signals were decomposed into single motor unit action potentials (MUAPs) by convolutive blind source separation (44, 50). This approach has been previously validated and guarantees high accuracy in the identification of motor unit discharges for the tibialis anterior muscle at least up to 70% MVC force (20, 35, 50). The decomposition accuracy was assessed with the silhouette measure (SIL) with a threshold of SIL> 0.90 (50). The double differential MUAP waveforms were extracted by spike averaging, triggered with the discharge timings of the decomposed motor units over intervals of 15 ms (Fig 1.D) (15). A custom MATLAB (Mathworks, Natic, MA) program was used to visually display the MUAPs in the two-dimensional array and a minimum of three up to a maximum of six channels were manually selected for each individual MUAP estimates (MUCV, MDF_{MU}, and RMS_{MU}). The EMG channel selection criterion for individual MUAP properties was the maximum cross-correlation between channels, as for the global EMG estimates. The channels automatically selected with this criterion were manually inspected. In a few cases, the action potentials were influenced by end-of-fiber components despite shape similarity and high cross-correlation. In these rare cases, the channels were manually re-selected to maximize propagation. Fig. 1D shows an example of motor unit action potential and channel selection for the computation of the motor unit properties (the channels highlighted in bold are selected for the analysis). MUCV, MDF_{MU} and RMS_{MU} were calculated with the same algorithms used for the global EMG estimates applied to the single motor unit action potentials (*see above*). Finally, the average motor unit discharge rate and voluntary force in ankle-dorsi-flexion (%MVC) were computed.

Regression analysis and statistics

Subject-specific correlations between global EMG and single motor unit variables with the respective joint torque were assessed with Pearson statistics. The slope of the regression lines between global EMG variables and joint torque (e.g., rate of change per %MVC) was correlated with the slope of the regression lines between motor unit variables and recruitment thresholds. The same procedure was used to assess the relations between the amplitude and power spectral frequencies to the rate of change in MUCV. Paired sample t-tests were used to assess differences in the intercepts between global and single motor unit properties. Statistical analyses were performed using MATLAB and statistical significance was accepted for P values smaller than 0.05. Results are reported as mean and standard deviation (SD).

RESULTS

HDEMG decomposition

The total number of decomposed motor units was 537 with an average of 41 (21) motor units per subject. The decomposition accuracy corresponded to an average SIL of 0.93 (0.02), indicating high accuracy in the identification of discharge timings. The mean discharge rate was 15.67 (4.75) pulses per second.

EMG variables and force

Global EMG estimates of conduction velocity and amplitude increased with force in all the tested subjects (R^2 mean, (SD) and [range], MFCV = 0.81 (0.12), [0.60-0.90], RMS_{GLO} = 0.88 (0.03), [0.82-0.94], p<0.001, Fig 2B, Table 1). Conversely, the median frequency of the interference EMG signal was correlated with force only in some subjects (R^2 = 0.27 (0.21) Table 1., Fig 3D). Moreover, when the median frequency was significantly associated with force, the correlation was very weak (Fig 3D, Table 1.).

At the motor unit level, the progressive recruitment of motor units corresponded to a linear increase in MUCV in all the tested subjects (R^2 = 0.64 (0.14) [0.41-0.94], p<0.001, Fig 3A, Table 1.). Conversely, the median frequency and amplitude of the motor unit action potentials showed highly variable strengths of correlation with motor unit recruitment thresholds (R^2 mean and (SD), MDF_{MU} = 0.11 (0.11), RMS_{MU} = 0.34 (0.29), Fig 2C,E). Moreover, in the cases when the amplitude and the spectral frequencies of individual motor unit action potentials were significantly correlated with recruitment thresholds, the relations were weak (Fig 2C,E, Table 1).

Subject-specific regression values (R^2, significance, intercepts, and slopes) of global variables when correlated with joint force and single motor unit variables with respect to motor unit recruitment thresholds are reported in the Tables 1-3.

Recruitment Thresholds and EMG variables

We studied the associations between the rate of change of motor unit variables with recruitment threshold and the rate of change in EMG global variables with joint force. For this purpose, the rate of change in motor unit variables as a function of recruitment thresholds was correlated with the rate of change in global EMG variables with respect to force. These relations indicate the level of association between motor unit recruitment and global EMG analysis.

The rate of change in the average conduction velocity of the action potentials along the muscle fibers (MFCV) predicted well the progressive increase in single motor unit conduction velocities with respect to motor unit recruitment thresholds (R^2 = 0.71, p<0.001, Fig 3A-C). The rate of change in global EMG median frequencies was also significantly correlated with the rate of change in single motor unit median frequency, but with a weaker relation (R^2 = 0.36, p<0.05, Fig 3B). A similar correlation was found when the EMG median frequency was correlated with the median frequency of individual motor unit action potentials from the bipolar electrodes (R^2 = 0.30; p=0.05).

The relations between amplitude of the surface EMG and the respective motor unit action potential amplitudes were highly variable (Fig 3C). For example, when subject #11 was removed from the correlation statistics between rate of change in EMG global amplitude and rate of change in the single motor unit amplitudes (Fig 3C), the Pearson P value was not significant (R^2 = 0.10, P = 0.30). The negative association between motor unit action potential amplitude and global EMG activity was due to the large variability in action potential amplitude when analyzed as a function of recruitment thresholds (Fig 2E). Similarly, global and single motor unit amplitudes from the large bipolar EMG were not correlated (R^2 = 0.01 p>0.05). Therefore, the monotonic increase in global EMG amplitude was not correlated to the progressive motor unit recruitment.

The amplitude and spectral frequencies of the EMG and of single motor unit action potentials were correlated with the rate of change in MUCV with respect to recruitment thresholds (Fig. 4. A-D). Interestingly, the rate of change in single motor unit median frequency was correlated with the rate of change in motor unit conduction velocity (Fig 4A, p<0.05), despite the fact that the increase the EMG spectral frequencies did not predict the changes in MUCV (Fig 4B, p>0.05). It is important to add that albeit the increase in single motor unit median frequency was correlated with the rate of change in MUCV, the relations between motor unit spectral estimates and recruitment thresholds were highly variable between subjects (Fig 2C, Table 1).

Further, the monotonic increase in global EMG amplitude did not relate to the progressive recruitment of motor units (p>0.05 Fig 4D) which agrees with the dissociation between the rate of change in global EMG amplitude and the rate of change in single motor unit amplitudes (see *Recruitment Thresholds and EMG variables*). Similarly, the rate of change in motor unit action potential amplitude was not correlated with the rate of change in MUCV (p>0.05, Fig 4B). These two variables were also not correlated when using the large bipolar EMG (p>0.05; R^2=0.01). Overall, the only global EMG variable that predicted the progressive recruitment of motor units was the rate of change in average muscle fiber conduction velocity (Fig 2.A-B Fig. 3.A). Moreover, the initial values for single motor unit conduction velocity and for the average muscle fiber conduction velocity were not statistically different (intercepts mean (SD), MUCV = 3.88 (0.35), MFCV = 3.77 (0.35) m/s; paired t-test, p<0.001, Table 2).

DISCUSSION

We have experimentally analyzed the relations between motor unit recruitment and global EMG variables. Global and single motor unit estimates were related with the respective motor unit properties during recruitment. The only variable that was positively associated with the progressive recruitment of motor units was the average conduction velocity of motor unit action potentials along the muscle fibers, as estimated from the interference EMG. Conversely, the amplitude and power spectral frequencies of the surface EMG signal were largely variable among subjects and not significantly correlated with motor unit recruitment.

Motor unit recruitment and global EMG estimates

Global EMG estimates have been extensively used for the analysis of the neuromuscular function. However, the interpretation of EMG features has also been debated (12, 24, 25, 51, 58), primarily due to the associations between characteristics of the interference EMG signal and motor unit behavior. For example, the power spectral frequencies have been used to infer MFCV and motor unit recruitment in several conditions (5, 40, 42, 46, 58, 61, 62), albeit these associations were demonstrated only for steady contractions (2). Similarly, the amplitude of the surface EMG is widely used to assess the neural drive to muscles, but the underlying contribution of single motor units to global EMG amplitude remains unclear. The challenges in interpretation of global EMG variables depend on the difficulty to experimentally identify large populations of motor units. Therefore, the relations between motor unit population behavior and global EMG estimates with respect to joint force were previously mainly based on simulation studies. Here, we assessed for the first time these relations experimentally for the full recruitment range of the tibialis anterior muscle. We assessed the properties of individual motor unit action potentials for interpreting the influence of motor unit behavior on the surface EMG features.

Conduction velocity

It has been previously suggested that the increase in MFCV during voluntary force contractions is related to progressive recruitment of larger, higher-threshold motor units (1). Following stimulation of single motor axons in the tibialis anterior muscle, a significant correlation between MUCV and motor unit mechanical properties was found (1). This strong correlation suggested that the propagation velocity of action potentials along muscle fibers can be considered as a size principle parameter (1). This result is due to the association between fiber diameter and conduction velocity (7, 29). However, due to classic technical limitations, it has not been possible to relate MUCV and recruitment thresholds for large populations of motor units.

In the present study, a strong correlation between MUCV and recruitment threshold was found. This association is in agreement with previous human and animal research that indirectly correlated the recruitment threshold of motor neurons to muscle fiber properties in the muscle units. Indeed, in human stimulation studies (1), during voluntary force contractions (10, 11, 22, 30, 45), and in animal studies (9, 29, 31, 32, 60), a strong correlation between size of the motor unit and motor unit mechanical properties has been observed. However, contrary to all previous research, this is first study that provides a systematic association between the voluntary recruitment of motor units and muscle unit property. The relation between recruitment threshold and MUCV reported in the present study underlies the association between spinal (motor neuron size) and muscular properties (muscle fiber diameters in muscle units) (8, 32, 33).

The study of MUCV requires the decomposition of a surface EMG signal, thus it is limited to controlled laboratory conditions, mainly in isometric slow-force contractions (20). Conversely, the average propagation velocity of action potentials along muscle fibers can be measured during a wide range of experimental conditions from the interference EMG (4, 18, 22, 53). The present study showed that the rate of change of average MFCV with respect to force is strongly correlated to the rate of change of individual motor unit MUCV with respect to recruitment thresholds (Fig 3. A.). This experimental observation implies that average MFCV during increasing force contractions can be used to assess the progressive recruitment of motor units. Despite MFCV has indeed been used for this purpose in dynamic exercises in previous studies, e.g., (4, 22, 53), the current study directly proves that the trends of MUCV can be predicted from the global analysis of the EMG by MFCV. Moreover, there was no difference in the initial value for MUCV and MFCV estimates. This observation confirms that the estimates of MFCV for low forces represents an accurate average of the conduction velocity of the lower threshold motor units, as indicated in Table 2.

Power spectral frequencies

The relations between EMG spectral variables and motor unit recruitment received substantial attention in the past decades (19, 42, 58, 62). Simulation and animal studies were conducted to investigate the association between EMG frequency components to the underlying motor unit activity (19, 40, 42, 58).

The use of EMG spectral analysis as a motor unit recruitment parameter is based on the theoretical prediction that the conduction velocity of an action potential scales the power spectrum of the action potential waveform (5, 19, 42, 46, 58). Further, previous research showed an association between MDF and MFCV during fatiguing contractions (2). However, when the power spectral frequencies were assessed during isometric linearly increasing force contractions, the results were largely different among studies. In some studies, MDF increased with force (48, 56), whilst in other it remained constant (38, 52), or even decreased (55, 63). In the present study, we report the same large variability among subjects as seen in previous studies (e.g., Table 1-3). These differences across subjects may be explained by the volume conductor and random position of muscle units within the muscle tissue. For example, a large, high-threshold motor unit with fibers located deep in the muscle may lower the frequency content of the EMG and cause a decrease in power spectral frequencies despite a high conduction velocity (e.g., Fig 1D-F).

When individual motor unit spectral variables were related to motor unit recruitment thresholds, a large variability between subjects was still found (Fig 4C). These results are in agreement with the theoretical and simulation predictions (19, 24, 25). Indeed, the association between conduction velocity and power spectral frequencies at the level of individual motor units is only valid for relative changes, such as those occurring during sustained fatiguing contractions, but not between different motor units, as directly proven experimentally in this study (Fig. 4A). Further, the interference EMG spectral frequencies were associated to the spectral frequencies of individual motor unit action potentials, as theoretically predicted. Indeed, the discharge rates of motor units have a smaller impact on the spectral components of the interference EMG than the shapes of the action potential waveforms (25), which explains the experimental association between single motor unit action potential and interference EMG spectral properties (Fig. 3B). These results indicate that the claims that the volume conductor effect does not impact the association between conduction velocity and EMG spectral properties (62) are not substantiated.

A significant correlation was found between the rate of change of single motor unit power spectral frequencies and that of MUCV (Fig. 4A) (19, 42). However, the correlation was weak and variable among subjects, indicating the effects of the volume conductor, discussed above, when making absolute rather than relative comparisons. Indeed, as a consequence of the high variability in single motor unit spectral frequencies (Fig 2. E Table 1), global EMG spectral frequencies did not correlate with torque consistently (Fig 2. D Table 1). This result clearly indicates that the relation between EMG spectral frequencies and force cannot be used to test differences in motor unit recruitment among subjects, during exercise/learning interventions or in pathology (34, 40, 41, 59, 61, 62). For example, the peak in EMG power spectral frequency during an increasing force contraction does not correspond to the end of motor unit recruitment, but rather depends on characteristics of the volume conductor and locations of the motor units in the muscle tissue.

Amplitude

EMG amplitude systematically increased with force in all subjects (Fig 2. F, Table 1), which is theoretically predicted (25) and well in agreement with a vast literature (e.g., 34, 37, 40, 44). However, at the single motor unit level, the amplitude of the motor unit action potentials showed a relation with force that differed greatly among subjects (Fig 2. E, Table 1). For example, the action potential of a motor unit recruited at 24.9% MVC shows a significant larger size when compared to a motor unit recruited at 63.9 % MVC (Figure 1D-F). Further, the rate of change in global EMG amplitude was only weakly correlated with the rate of change in single motor unit action potential amplitudes with recruitment threshold (Fig 4. C), as it was anticipated in previous simulations studies (17, 37). For example, in Fig. 1, the motor unit recruited at 24% MVC had an action potential with greater amplitude compared to the higher threshold motor unit recruited at 64% MVC. These associations between the size of the motor unit action potential and the EMG amplitude suggest that the amplitude of the EMG signal does not only reflect recruitment and therefore it is not indicative of a specific recruitment order. Indeed, the increase in the interference EMG amplitude would be observed with any type of recruitment strategy due to the monotonic increase in the discharge rate of motor units with force. Further, motor unit synchronization also influences the relation between EMG amplitude and motor unit action potentials, as previously shown in simulation studies (64). The weak associations between EMG amplitude and progressive motor unit recruitment previously reported in several simulation studies and now experimentally shown in large populations of motor units further strengthen the evidence that global and motor unit EMG amplitude should not be used to test the neural strategies of muscle control.

Conclusion

We have identified large populations of motor units by using high-density EMG techniques and we have associated the motor unit properties to force and to the features of the interference EMG. The results have clarified in a direct experimentally way the nature and strengths of long-discussed associations between properties of the interference EMG and the neural strategies of muscle control. Whereas the spectral properties of the surface EMG did not correlate reliably with motor unit recruitment, the average conduction velocity of action potentials as estimated from the interference EMG was a good predictor of motor unit recruitment. This association may be used for inferring recruitment strategies in conditions when a full EMG decomposition into individual motor unit activity is not possible, such as in fast dynamic tasks. Conversely, the use of spectral EMG analysis for inferring recruitment strategies should be abandoned.

Reference

1. **Andreassen S**, **Arendt-Nielsen L**. Muscle fibre conduction velocity in motor units of the human anterior tibial muscle: a new size principle parameter. *J Physiol* 391: 561–571, 1987.

2. **Arendt-Nielsen L**, **Mills K.** The relationship between mean power frequency of the EMG spectrum and muscle fibre conduction velocity. *Electroencephalogr Clin Neurophysiol* 60: 130–134, 1985.

3. **Arendt-Nielsen L**, **Zwarts MJ**. Measurement of Muscle Fiber Conduction Velocity in Humans: Techniques and Applications. *J Clin Neurophysiol* 6: 173–190, 1989.

4. **Bazzucchi I**, **De Vito G**, **Felici F**, **Dewhurst S**, **Sgadari A**, **Sacchetti M**. Effect of exercise training on neuromuscular function of elbow flexors and knee extensors of type 2 diabetic patients. *J Electromyogr Kinesiol* 25: 815–823, 2015.

5. **Bernardi M**, **Solomonow M**, **Nguyen G**, **Smith A**, **Baratta R**. Motor unit recruitment strategy changes with skill acquisition. *Eur J Appl Physiol Occup Physiol* 74: 52–59, 1996.

6. **Bigland-Ritchie B**, **Donovan EF**, **Roussos CS**. Conduction velocity and EMG power spectrum changes in fatigue of sustained maximal efforts. *J Appl Physiol* 51: 1300–1305, 1981.

7. **Blijham PJ**, **ter Laak HJ**, **Schelhaas HJ**, **van Engelen BGM**, **Stegeman DF**, **Zwarts MJ**. Relation between muscle fiber conduction velocity and fiber size in neuromuscular disorders. *J Appl Physiol* 100: 1837–1841, 2006.

8. **Burke RE**. Motor units: anatomy, physiology, and functional organization. *Handb Physiol - Nerv Syst* 543: 345–422, 2011.

9. **Burke RE**, **Levine DN**, **Tsairis P**, **Zajac FE**. Physiological types and histochemical profiles in motor units of the cat gastrocnemius. *J Physiol* 234: 723–748, 1973.

10. **Van Cutsem M**, **Duchateau J**, **Hainaut K**. Changes in single motor unit behaviour contribute to the increase in contraction speed after dynamic training in humans. *J Physiol* 513: 295–305, 1998.

11. **Van Cutsem M**, **Feiereisen P**, **Duchateau J**, **Hainaut K**. Mechanical properties and behaviour of motor units in the tibialis anterior during voluntary contractions. *Can J Appl Physiol* 22: 585–597, 1997.

12. **Enoka RM**, **Duchateau J**. Inappropriate interpretation of surface EMG signals and muscle fiber characteristics impedes progress on understanding the control of neuromuscular function. *J Appl Physiol* 119: 1516–1518, 2015.

13. **Farina D**. Counterpoint: Spectral properties of the surface EMG do not provide information about motor unit recruitment and fiber type. *J Appl Physiol* 105: 1673–1674, 2008.

14. **Farina D**, **Arendt-Nielsen L**, **Graven-Nielsen T**. Effect of temperature on spike-triggered average torque and electrophysiological properties of low-threshold motor units. *J Appl Physiol* 99: 197–203, 2005.

15. **Farina D**, **Arendt-Nielsen L**, **Merletti R**, **Graven-Nielsen T**. Assessment of single motor unit conduction velocity during sustained contractions of the tibialis anterior muscle with advanced spike triggered averaging. *J Neurosci Methods* 115: 1–12, 2002.

16. **Farina D**, **Arendt-Nielsen L**, **Merletti R**, **Graven-Nielsen T**. Effect of experimental muscle pain on motor unit firing rate and conduction velocity. .

17. **Farina D**, **Cescon C**, **Negro F**, **Enoka RM**. Amplitude Cancellation of Motor-Unit Action Potentials in the Surface Electromyogram Can Be Estimated With Spike-Triggered Averaging. *J Appl Physiol* 100: 431–400, 2008.

18. **Farina D**, **Ferguson RA**, **Macaluso A**, **De Vito G**. Correlation of average muscle fiber conduction velocity measured during cycling exercise with myosin heavy chain composition, lactate threshold, and VO2max. *J Electromyogr Kinesiol* 17: 393–400, 2007.

19. **Farina D**, **Fosci M**, **Merletti R**. Motor unit recruitment strategies investigated by surface EMG variables.

J Appl Physiol 92: 235–247, 2002.

20. **Farina D**, **Holobar A**. Characterization of Human Motor Units from Surface EMG Decomposition. *Proc IEEE* 104: 353–373, 2016.

21. **Farina D**, **Holobar A**, **Merletti R**, **Enoka RM**. Decoding the neural drive to muscles from the surface electromyogram. *Clin Neurophysiol* 121: 1616–1623, 2010.

22. **Farina D**, **Macaluso A**, **Ferguson RA**, **De Vito G**. Effect of power, pedal rate, and force on average muscle fiber conduction velocity during cycling. *J Appl Physiol* 97: 2035–2041, 2004.

23. **Farina D**, **Merletti R**. Comparison of algorithms for estimation of EMG variables during voluntary isometric contractions. *J Electromyogr Kinesiol* 10: 337–349, 2000.

24. **Farina D**, **Merletti R**, **Enoka RM**. The extraction of neural strategies from the surface EMG. *J Appl Physiol* 96: 1486–1495, 2004.

25. **Farina D**, **Merletti R**, **Enoka RM**. The extraction of neural strategies from the surface EMG: an update. *J Appl Physiol* 117: 1215–1230, 2014.

26. **Farina D**, **Muhammad W**, **Fortunato E**, **Meste O**, **Merletti R**, **Rix H**. Estimation of single motor unit conduction velocity from surface electromyogram signals detected with linear electrode arrays. *Med Biol Eng Comput* 39: 225–236, 2001.

27. **Farina D**, **Negro F**, **Muceli S**, **Enoka RM**. Principles of motor unit physiology evolve with advances in technology. *Physiology* 31: 83–94, 2016.

28. **González-Izal M**, **Malanda A**, **Gorostiaga E**, **Izquierdo M**. Electromyographic models to assess muscle fatigue. *J Electromyogr Kinesiol* 22: 501–512, 2012.

29. **Håkansson CH**. Conduction Velocity and Amplitude of the Action Potential as Related to Circumference in the Isolated Fibre of Frog Muscle. *Acta Physiol Scand* 37: 14–34, 1956.

30. **Heckman CJ**, **Enoka RM**. Motor Unit. *Compr Physiol* 2: 2629–2682, 2012.

31. **Henneman E**. Relation between size of neurons and their susceptibility to discharge. *Science* 126: 1345–7, 1957.

32. **Henneman E**, **Olson C**. Relations between structure and function in the design of skeletal muscles. *J Neurophysiol* 28: 581–598, 1965.

33. **Henneman E**, **Somjen G**, **Carpenter DO**. Functional Significance of Cell Size in Spinal Motoneurons. *J Neurophysiol* 28: 560–580, 1965.

34. **Herda T**, **Siedlik J**, **Trevino M**, **Cooper M**, **Weir J**. Motor unit control strategies of endurance versus resistance trained individuals. *Muscle Nerve* : 1–23, 2015.

35. **Holobar A**, **Minetto M a**, **Farina D**. Accurate identification of motor unit discharge patterns from high-density surface EMG and validation with a novel signal-based performance metric. *J Neural Eng* 11: 16008, 2014.

36. **Holtermann A**, **Roeleveld K**. EMG amplitude distribution changes over the upper trapezius muscle are similar in sustained and ramp contractions. *Acta Physiol* 186: 159–168, 2006.

37. **Keenan KG**, **Farina D**, **Merletti R**, **Enoka RM**. Amplitude cancellation reduces the size of motor unit potentials averaged from the surface EMG. *J Appl Physiol* 100: 1928–1937, 2006.

38. **Komi P V.**, **Viitasalo JHT**. Signal Characteristics of EMG at Different Levels of Muscle Tension. *Acta Physiol Scand* 96: 267–276, 1976.

39. **Lawrence JH**, **De Luca CJ**. Myoelectric signal versus force relationship in different human muscles. *J Appl Physiol* 54: 1653–1659, 1983.

40. **Lee SSM**, **de Boef Miara M**, **Arnold AS**, **Biewener AA**, **Wakeling JM**. EMG analysis tuned for

determining the timing and level of activation in different motor units. *J Electromyogr Kinesiol* 21: 557–565, 2011.

41. **Li X**, **Shin H**, **Zhou P**, **Niu X**, **Liu J**, **Rymer WZ**. Power spectral analysis of surface electromyography (EMG) at matched contraction levels of the first dorsal interosseous muscle in stroke survivors. *Clin Neurophysiol* 125: 988–994, 2014.

42. **Lindström LH**, **Magnusson RI**. Interpretation of Myoelectric Power Spectra: A Model and Its Applications. *Proc IEEE* 65: 653–662, 1977.

43. **Lippold OCJ**. The relation between integrated action potentials in a human muscle and its isometric tension. *J Physiol* 117: 492–499, 1952.

44. **Martinez-Valdes E**, **Negro F**, **Laine CM**, **Falla D**, **Mayer F**, **Farina D**. Tracking motor units longitudinally across experimental sessions with high-density surface electromyography. *J Physiol* 44, 2016.

45. **Masuda T**, **De Luca CJ**. Recruitment threshold and muscle fiber conduction velocity of single motor units. *J Electromyogr Kinesiol* 1: 116–123, 1991.

46. **Merletti R**, **Knaflitz M**, **De Luca CJ**. Myoelectric manifestations of fatigue in voluntary and electrically elicited contractions. *J Appl Physiol* 69: 1810–1820, 1990.

47. **Milner-Brown HS**, **Stein RB**. The relation between the surface electromyogram and muscular force. *J Physiol* 246: 549–569, 1975.

48. **Moritani T**, **Muro M**. Motor unit activity and surface electromyogram power spectrum during increasing force of contraction. *Eur J Appl Physiol* 56: 260–265, 1987.

49. **Muceli S**, **Poppendieck W**, **Negro F**, **Yoshida K**, **Hoffmann KP**, **Butler JE**, **Gandevia SC**, **Farina D**. Accurate and representative decoding of the neural drive to muscles in humans with multi-channel intramuscular thin-film electrodes. *J Physiol* 17: 3789–3804, 2015.

50. **Negro F**, **Muceli S**, **Castronovo AM**, **Holobar A**, **Farina D**. Multi-channel intramuscular and surface EMG decomposition by convolutive blind source separation. *J Neural Eng* 13: 26027, 2016.

51. **Neyroud D**, **Kayser B**, **Place N**. Commentaries on Viewpoint : Inappropriate interpretation of surface EMG signals and muscle fiber characteristics impedes understanding of the control of neuromuscular function. *J Appl Physiol* 119: 8750, 2015.

52. **Petrofsky JS**, **Lind AR**. Frequency analysis of the surface electromyogram during sustained isometric contractions. *Eur J Appl Physiol* 43: 173–182, 1980.

53. **Pozzo M**, **Merlo E**, **Farina D**, **Antonutto G**, **Merletti R**, **Di Prampero PE**. Muscle-fiber conduction velocity estimated from surface EMG signals during explosive dynamic contractions. *Muscle and Nerve* 29: 823–833, 2004.

54. **Qi L**, **Wakeling JM**, **Green A**, **Lambrecht K**, **Ferguson-Pell M**. Spectral properties of electromyographic and mechanomyographic signals during isometric ramp and step contractions in biceps brachii. *J Electromyogr Kinesiol* 21: 128–135, 2011.

55. **Rainoldi A**, **Galardi G**, **Maderna L**, **Comi G**, **Lo Conte L**, **Merletti R**. Repeatability of surface EMG variables during voluntary isometric contractions of the biceps brachii muscle. *J Electromyogr Kinesiol* 9: 105–119, 1999.

56. **Sbriccoli P**, **Bazzucchi I**, **Rosponi A**, **Bernardi M**, **De Vito G**, **Felici F**. Amplitude and spectral characteristics of biceps Brachii sEMG depend upon speed of isometric force generation. *J Electromyogr Kinesiol* 13: 139–147, 2003.

57. **da Silva RA**, **Vieira ER**, **Cabrera M**, **Altimari LR**, **Aguiar AF**, **Nowotny AH**, **Carvalho AF**, **Oliveira MR**. Back muscle fatigue of younger and older adults with and without chronic low back pain using two protocols: A case-control study. *J Electromyogr Kinesiol* 25: 928–936, 2015.

58. **Solomonow M**, **Baten C**, **Smit J**, **Baratta R**, **Hermens H**, **D'Ambrosia R**, **Shoji H**. Electromyogram

power spectra frequencies associated with motor unit recruitment strategies. *J Appl Physiol* 68: 1177–1185, 1990.

59. **Tillin NA**, **Jimenez-Reyes P**, **Pain MTG**, **Folland JP**. Neuromuscular performance of explosive power athletes versus untrained individuals. *Med Sci Sports Exerc* 42: 781–790, 2010.

60. **Tötösy de Zepetnek JE**, **Zung H V**, **Erdebil S**, **Gordon T**. Innervation ratio is an important determinant of force in normal and reinnervated rat tibialis anterior muscles. *J Neurophysiol* 67: 1385–403, 1992.

61. **von Tscharner V**, **Nigg BM**. Spectral properties of the surface EMG can characterize /do not provide information about motor unit recruitment strategies and muscle fiber type. *J Appl Physiol* : 1671–1673, 2008.

62. **Wakeling JM**. Patterns of motor recruitment can be determined using surface EMG. *J Electromyogr Kinesiol* 19: 199–207, 2009.

63. **Westbury J**, **Shaughness T**. Associations between spectral representation of the surface electromyogram and fiber type distribution and size in human masseter muscle. *Electroencephalogr Clin Neurophysiol* 27: 427–35, 1987.

64. **Yao W**, **Fuglevand RJ**, **Enoka RM**. Motor-unit synchronization increases EMG amplitude and decreases force steadiness of simulated contractions. *J Neurophysiol* 83: 441–452, 2000.

Figure captions

Fig. 1. A. Example of an isometric linearly increasing (ramp) contraction (black line) up to 70% of maximal voluntary force (MVC). Eight surface EMG signals from one column of the matrix are reported (inter-electrode distance 8 mm). Clear increase in the EMG activity as the muscle is generating force can be observed. **B.** An example of two EMG time windows (500 ms) used for the extraction of global EMG features. Clear propagation of several motor unit action potentials (MUAPs) can be observed. **C.** High-density surface grids (64 electrodes, gold-coated). The motor unit comprising the EMG signal were decomposed into single MUAP trains and successively the first 50 discharge timings were used to trigger the MUAP signatures in the high-density surface electromyogram. **D.** The signature of a motor unit propagating in the matrix recruited at 24.9 % MVC can be seen. The lower left column of the matrix is removed in order to improve figure clarity. **E-F.** A low and high threshold motor unit propagating in the matrix. Only the column of the matrix which corresponded to clearest MUAP propagation is reported. The high threshold MUAP propagates at a greater velocity with respect to the low threshold motor unit. Moreover, the motor unit recruited at 24.9% MVC (**D**) has action potentials with greater amplitude with respect to the high threshold motor unit (**F**). The action potentials highlighted in bold correspond to the channels selected for the estimates of CV, MDF and RMS (**D-F**). (*RT = Recruitment Thresholds, *CV = motor unit conduction velocity, *MDF = median frequency, *RMS = root mean square).

Fig. 2. A. Motor unit conduction velocities (MUCV, m/s) plotted as a function of recruitment thresholds (%MVC, 537 motor units), $p<0.001$. **B.** The average muscle fiber conduction velocity (MFCV, m/s) plotted against the respective voluntary force, $p<0.001$. **C.** Individual motor unit median frequencies (MDF_{MU}, Hz) plotted as a function of motor unit recruitment thresholds (%). **D.** The average power spectra estimate of the interference EMG (MDF_{GLO}, Hz), signal plotted against muscular force. **E.** Single motor unit amplitudes (RMS_{MU}, μV) plotted as a function of recruitment thresholds **F.** Global EMG (RMS_{GLO}, μV) amplitude against the respective voluntary force, $p<0.001$. Each color corresponds to a specific subject. R^2 mean and (standard deviation) for each subject are given.

Fig. 3. A. Fig. 3. A. The rate of change in the average muscle fiber conduction velocity derived from the global EMG signal (slope of the regression line between conduction velocity and force) is reported as a function of the

rate of change of single motor unit conduction velocities (e.g., slope of the regression line between motor unit conduction velocity and recruitment threshold). **B.** The rate of change in the interference EMG median frequencies per percentages of MVC plotted against the rate of change in single motor unit median frequencies per percentages of motor unit recruitment thresholds. **C.** The rate of change in global EMG amplitudes per percentages of MVC as a function of the rate of change in single motor unit amplitudes per percentages of recruitment thresholds. Each color corresponds to a specific subject. ** = $p<0.001$, * = $p<0.05$.

Fig. 4. A-B. The rate of change in single motor unit spectral frequencies (MDF) and amplitudes (RMS), (e.g., slope of the MDF and RMS regression lines per percentages of Recruitment Thresholds) was plotted against the rate of change in single motor unit conduction velocities (MUCV) (e.g., slope of the regression lines per percentages of Recruitment Thresholds). **C-D** The rate of change in global interference EMG median frequencies (e.g., slope of the global MDF and RMS regression lines was correlated with the rate of change in single motor unit conduction velocities). Each color corresponds to a specific subject. * = $p<0.05$.

Table 1. Subject-specific coefficient of correlations (R^2) values. Motor unit variables were correlated with recruitment thresholds in percentages of MVC. Global EMG variables were correlated with force in percentages of MVC. * = p<0.001, # = p<0.05.

R^2 VALUES

	MOTOR UNIT			**GLOBAL EMG**		
SUBJECTS	MUCV	MDF_{MU}	RMS_{MU}	MFCV	MDF_{GLO}	RMS_{GLO}
S1	0.80*	0.01	0.20*	0.95*	0.21*	0.95*
S2	0.56*	0.06	0.25*	0.67*	0.03	0.92*
S3	0.54*	0.01	0.50*	0.63*	0.01	0.83*
S4	0.72*	0.20*	0.09*	0.84*	0.36*	0.87*
S5	0.56*	0.10	0.50*	0.84*	0.50*	0.82*
S6	0.51*	0.01	0.03	0.67*	0.01	0.90*
S7	0.56*	0.01	0.74*	0.88*	0.47*	0.89*
S8	0.82*	0.28*	0.52*	0.92*	0.61*	0.91*
S9	0.73	0.09	0.47*	0.89*	0.48*	0.89*
S10	0.80*	0.07#	0.20*	0.93*	0.31*	0.92*
S11	0.55*	0.32*	0.87*	0.90*	0.36*	0.89*
S12	0.86*	0.26*	0.54*	0.90*	0.17*	0.85*
S13	0.41*	0.15	0.28	0.61*	0.01	0.90*

Table 2. Subject-specific intercepts values. Motor unit intercepts values represent the initial value from the regression line between motor unit variables and motor unit recruitment thresholds. Global EMG variables intercepts corresponded to the initial value of the regression line between global EMG and muscular force in percentages of MVC.

INTERCEPTS						
	MOTOR UNIT			**GLOBAL EMG**		
SUBJECTS	MUCV (m/s)	MDF_{MU} (Hz)	RMS_{MU} (µV)	MFCV (m/s)	MDF_{GLO} (Hz)	RMS_{GLO} (µV)
S1	3.793	134.868	63.376	3.738	132.471	5.015
S2	3.584	108.072	55.103	3.918	110.079	18.764
S3	4.282	120.640	32.560	4.435	123.319	58.977
S4	3.587	119.533	105.992	3.442	121.254	31.443
S5	3.588	102.486	60.297	3.634	84.510	-6.395
S6	3.381	101.209	56.862	3.306	103.656	14.365
S7	4.053	122.173	32.157	3.852	96.414	15.093
S8	3.420	125.267	27.418	3.526	131.277	-1.449
S9	4.013	134.561	74.794	3.747	144.157	10.200
S10	4.122	131.963	90.956	4.105	125.581	64.998
S11	4.107	94.587	-31.383	3.508	114.483	21.821
S12	3.999	112.704	81.070	3.513	115.206	68.617
S13	4.544	117.058	45.584	4.414	107.237	52.707

Table 3. Subject-specific rate of change in motor unit and global EMG variables when correlated as a function of either recruitment thresholds or force (e.g., regression slope values per percentages of MVC).

SLOPES						
	MOTOR UNIT			**GLOBAL EMG**		
SUBJECTS	MUCV ($ms^{-1}\cdot m$)	MDF_{MU} ($Hz\cdot m$)	RMS_{MU} ($\mu V\cdot m$)	MFCV ($ms^{-1}\cdot m$)	MDF_{GLO} ($Hz\cdot m$)	RMS_{GLO} ($\mu V\cdot m$)
S1	0,0298	0,0582	1,8447	0,0199	0,2560	3,3144
S2	0,0257	0,2439	1,0237	0,0160	-0,0876	4,4956
S3	0,0107	0,0851	1,6576	0,0103	0,0418	2,3394
S4	0,0317	0,6936	1,4838	0,0248	0,5106	10,3813
S5	0,0213	0,5128	2,3284	0,0164	0,8043	3,8474
S6	0,0133	0,0617	0,2487	0,0076	0,0122	3,0981
S7	0,0171	0,0247	2,3670	0,0200	0,5891	3,9997
S8	0,0315	0,7197	1,0229	0,0255	0,6347	2,6126
S9	0,0254	0,3695	2,5481	0,0218	0,5461	8,2577
S10	0,0253	0,3307	1,8686	0,0184	0,4275	7,7520
S11	0,0219	1,0658	9,8523	0,0233	0,4647	10,5602
S12	0,0251	0,5058	3,0181	0,0206	0,3051	5,8349
S13	0,0120	-0,4552	1,3994	0,0070	-0,0555	2,8302

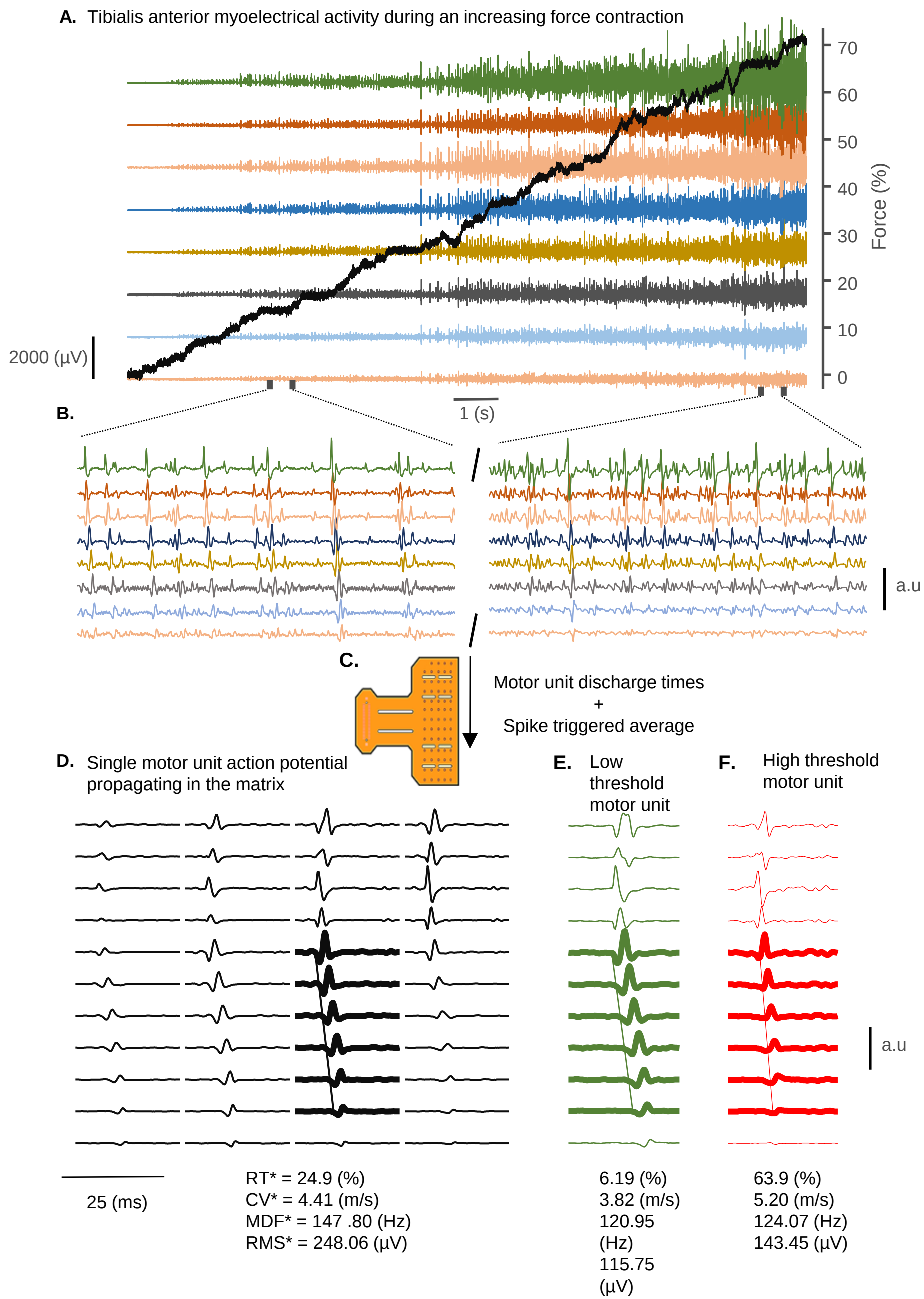
A. Tibialis anterior myoelectrical activity during an increasing force contraction
70
60
50
40
30
20
10
0
Force (%)
2000 (µV)
1 (s)
B.
a.u
C.
Motor unit discharge times
+
Spike triggered average
D. Single motor unit action potential propagating in the matrix
E. Low threshold motor unit
F. High threshold motor unit
a.u
25 (ms)
RT* = 24.9 (%)
CV* = 4.41 (m/s)
MDF* = 147 .80 (Hz)
RMS* = 248.06 (µV)
6.19 (%)
3.82 (m/s)
120.95 (Hz)
115.75 (µV)
63.9 (%)
5.20 (m/s)
124.07 (Hz)
143.45 (µV)

Fig. 1.

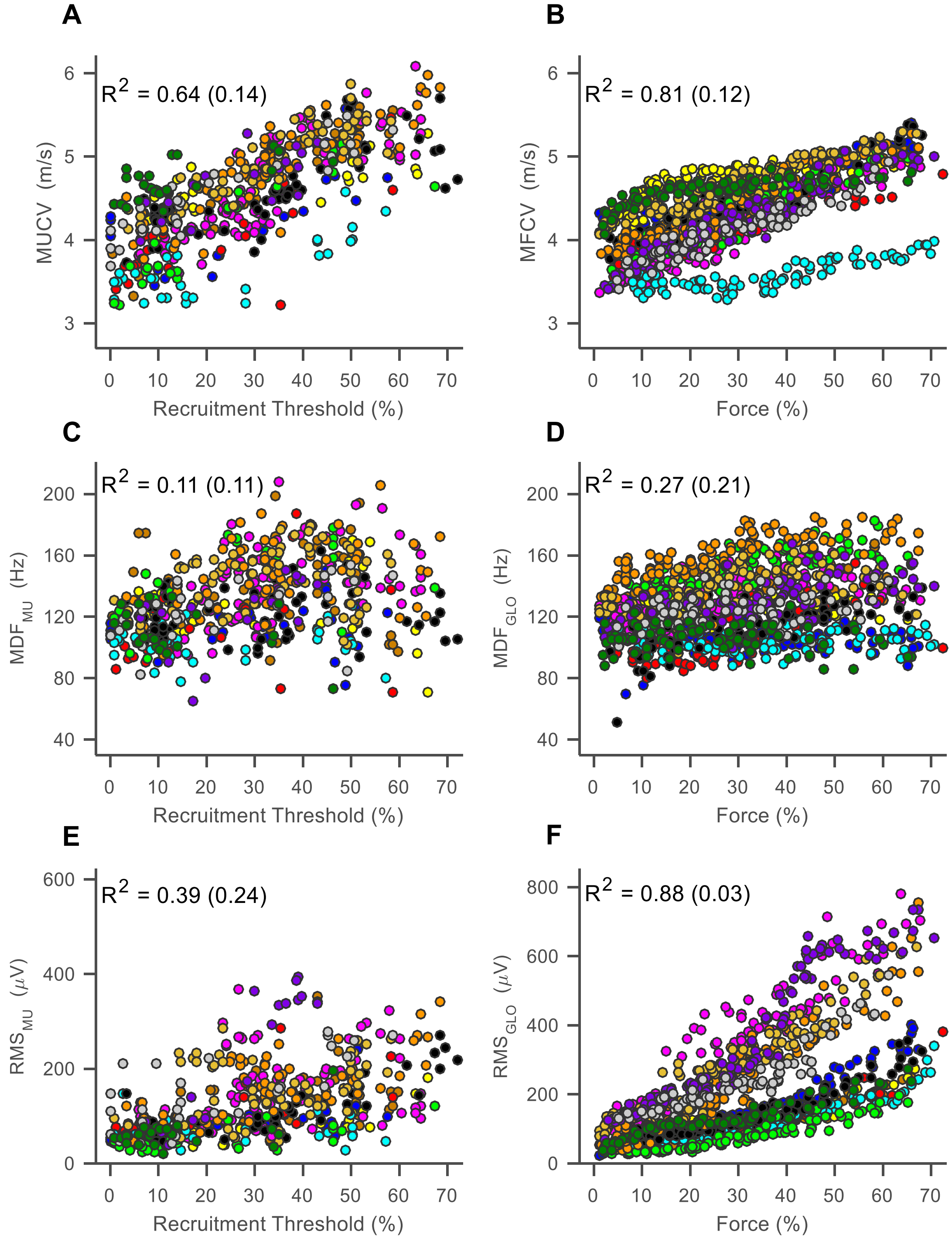
A
R2 = 0.64 (0.14)
MUCV (m/s)
Recruitment Threshold (%)
B
R2 = 0.81 (0.12)
MFCV (m/s)
Force (%)
C
R2 = 0.11 (0.11)
MDFMU (Hz)
Recruitment Threshold (%)
D
R2 = 0.27 (0.21)
MDFGLO (Hz)
Force (%)
E
R2 = 0.39 (0.24)
RMSMU (μV)
Recruitment Threshold (%)
F
R2 = 0.88 (0.03)
RMSGLO (μV)
Force (%)

Fig. 2.

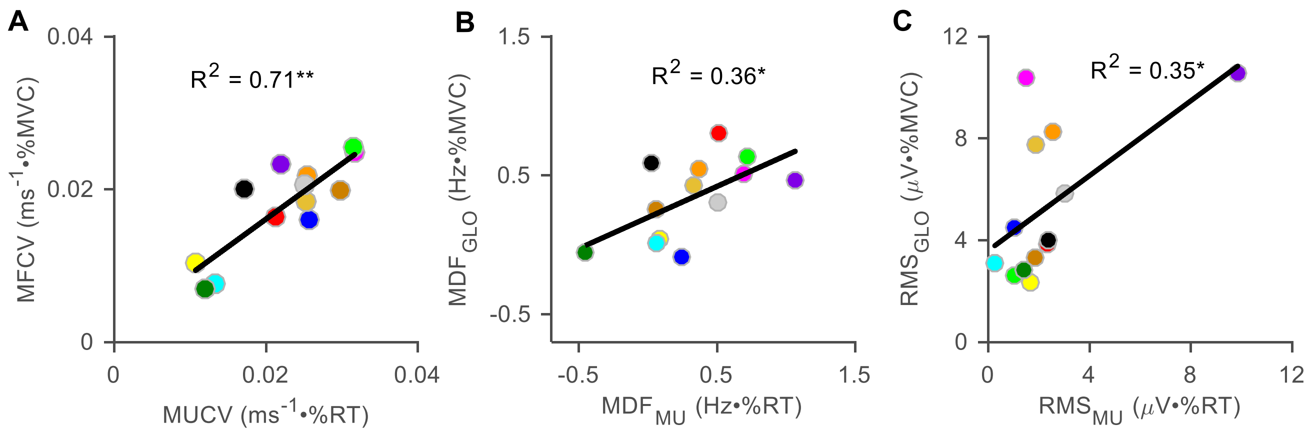

A
0.04
0.02
0
MFCV (ms-1•%MVC)
R^2 = 0.71**
0
0.02
0.04
MUCV (ms-1•%RT)
B
1.5
0.5
-0.5
MDFGLO (Hz•%MVC)
R^2 = 0.36*
-0.5
0.5
1.5
MDFMU (Hz•%RT)
C
12
8
4
0
RMSGLO (μV•%MVC)
R^2 = 0.35*
0
4
8
12
RMSMU (μV•%RT)

Fig. 3.

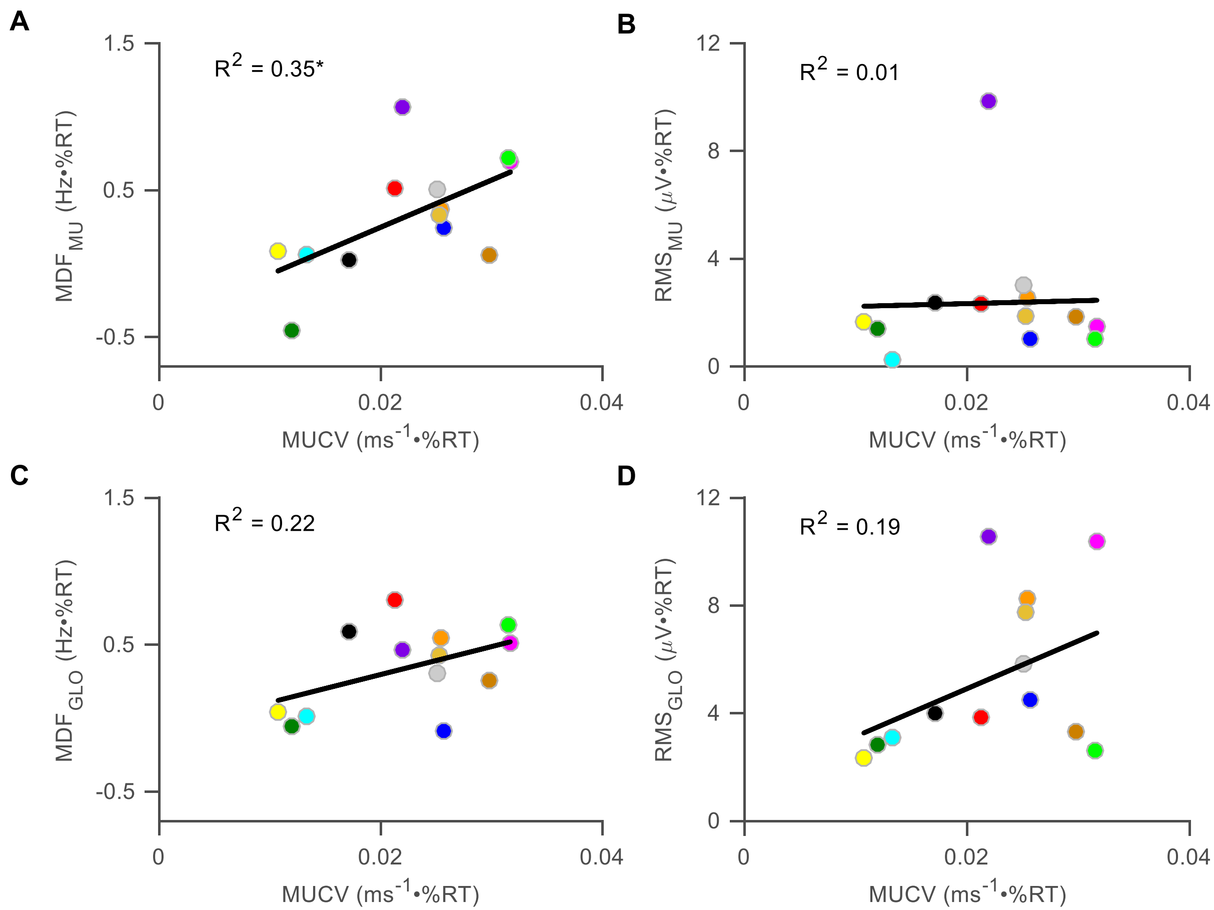

A
B
C
D
R2 = 0.35*
R2 = 0.01
R2 = 0.22
R2 = 0.19
MDFMU (Hz•%RT)
RMSMU (μV•%RT)
MDFGLO (Hz•%RT)
RMSGLO (μV•%RT)
MUCV (ms-1•%RT)
1.5
0.5
-0.5
12
8
4
0
0.02
0.04

Fig. 4.